Carbon nanotubes band assignation, topology, Bloch states, and selection rules

T. Vuković,* I. Milošević, and M. Damnjanović
Faculty of Physics, University of Belgrade, P.O. Box 368, Beograd 11001, Yugoslavia
(Received 14 December 2000; revised manuscript received 13 September 2001; published 8 January 2002)

Various properties of the energy band structures (electronic, phonon, etc.), including systematic band degeneracy, sticking and extremes, following from the full line group symmetry of the single-wall carbon nanotubes are established. The complete set of quantum numbers consists of the angular and linear quasimomenta and parities with respect to the U axis and, for achiral tubes, the mirror planes. The assignation of the electronic bands is performed, and the generalized Bloch symmetry adapted eigen functions are derived. The most important physical tensors are characterized by the quantum numbers. All this enables application of the presented exhaustive selection rules. The results are discussed by some examples, e.g., allowed interband transitions, conductivity, Raman tensor, etc.

DOI: 10.1103/PhysRevB.65.045418 PACS number(s): 71.20.Tx, 63.22.+m, 61.48.+c

I. INTRODUCTION

It is well known that single-wall carbon nanotubes[1] (SWCT's), in addition to the translational periodicity along the tube axis (z axis, by convention), possess a screw axis and pure rotational symmetries. Consequently, in calculations of the electronic energy band structure the conserved quantum numbers of linear[2] k, or helical[3] $\tilde{k}$, quasimomenta together with z projection of the orbital angular momentum (related to rotational symmetries) are used. On the contrary, the parity quantum numbers following from the full line group symmetry[4] including horizontal U axis and, in the zig-zag and armchair cases, vertical and horizontal mirror and glide planes, have not been used in band assignation. It is important to complete this task, since it yields many important exact properties of the electronic band structures, some of them being quite independent of the model considered. Let us mention only the band degeneracies, systematic van Hove singularities and the precise selection rules relevant for the processes in nanotubes. Further, some general predictions on the topology of band sticking may be a priori predicted.

All the geometrical symmetries of chiral (n_1,n_2), zig-zag $(n,0)$, and armchair (n,n) SWCT's ($\mathcal{C}$, $\mathcal{Z}$, and $\mathcal{A}$ tubes for short) are gathered in the line groups[4] (the factorized and the international notation are given):

$$\mathbf{L}_{\mathcal{C}}=\mathbf{T}_q^r\mathbf{D}_n=\mathbf{L}q_p22, \tag{1a}$$

$$\mathbf{L}_{\mathcal{ZA}}=\mathbf{T}_{2n}^1\mathbf{D}_{nh}=\mathbf{L}2n_n/mcm. \tag{1b}$$

Here, n is the greatest common divisor of n_1 and n_2, $q=2(n_1^2+n_1n_2+n_2^2)/n\mathcal{R}$ with $\mathcal{R}=3$ or $\mathcal{R}=1$ whether $(n_1-n_2)/3n$ is integer or not, while the helicity parameters r and p are expressed in terms of n_1 and n_2 by number theoretical functions.[5] The elements of the groups (1) are (the coordinate system and the positions of the symmetry axes and planes are presented in Fig. 1):

$$l(t,s,u,v)=(C_q^r|na/q)^tC_n^sU^u\sigma_x^v, \tag{2}$$

where $(C_q^r|na/q)^t$ (Koster-Seitz notation; a is the translational period of the tube) for $t=0,\pm1,...$, are the elements of the helical group (screw axis) $\mathbf{T}_q^r$. The rotations C_n^s, $s=0,...,n-1$, around the z axis form the subgroup $\mathbf{C}_n$. Finally, U is the rotation by π around the x axis $(u=0,1)$, and σ_v the vertical mirror xz plane in the case of the achiral tubes, i.e., $v=0$, 1 for $\mathcal{Z}$ and $\mathcal{A}$ tubes, and $v=0$ for $\mathcal{C}$ ones. Each carbon atom on the tube is obtained from a single one C_{000} by the action of the element $l(t,s,u,0)$. This enables us to enumerate the atoms as C_{tsu}. The isogonal point groups are

$$\mathbf{P}_{\mathcal{C}}=\mathbf{D}_q, \quad \mathbf{P}_{\mathcal{ZA}}=\mathbf{D}_{2nh}. \tag{3}$$

The electronic eigen states (in the form of the generalized Bloch functions) and eigenenergies (organized as the energy bands) are assigned by the complete set of the symmetry based quantum numbers in Sec. II. The derived general tight-binding dispersion relations are considered also in the simplest approximation. Then, in Sec. III, the general forms of various tensors (e.g., dielectric permeability, Raman, conductivity) are presented, enabling application of the selection rules (given in the Appendix in the analysis of different processes. Basic conclusions are reviewed in the last section.

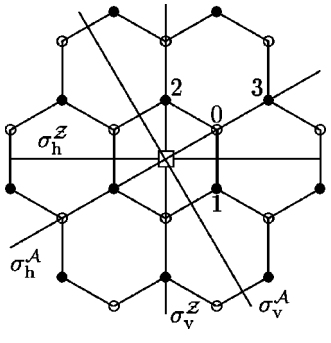

FIG. 1. Symmetry and neighbors. Perpendicular to the figure at □ is the U axis (assumed to be the x axis), while $\sigma_{h/v}^{\mathcal{Z}/\mathcal{A}}$ stands for vertical and horizontal mirror planes of $\mathcal{Z}$ and $\mathcal{A}$ tubes. Atoms C_{ts0} and C_{ts1} are differed as ○ and ●. Nearest neighbors of the atom C_{000}, denoted by 0, are the atoms 1, 2, and 3.

II. ELECTRONIC π BANDS

At first, we consider briefly the degeneracy of the bands imposed by the symmetry. Among two sets of quantum numbers used in literature for the chiral tubes,[6–8] we use the one related to the linear and total angular momenta. A state of (quasi)particle propagating along the z axis with the quasi momentum k and the z component of the angular momentum m is denoted as $|km\rangle$, or $|km\pm\rangle$. The parities invoked by U axis and, for the achiral tubes, mirror planes, combine these states in the degenerate multiplets, related to irreducible representations of the group (A or B for singlet, E for dublet, and G for quadruplet).

As for $\mathcal{C}$ tubes, m takes on the integer values from $(-q/2,q/2]$. All the equalities in k and m are assumed modulo these intervals. Due to U-axis symmetry, the states $|km\rangle$ and $|-k,-m\rangle$ form degenerate doublet for any $k \in (0,\pi/a)$, making a double degenerate band. At the point $k=0$, for $m=0$, $q/2$ there are nondegenerate even and odd states, $|00\pm\rangle$ and $|0,q/2,\pm\rangle$. For p even, at $k=\pi/a$ there are additional singlets $|\pi,-p/2,\pm\rangle$ and $|\pi,(q-p)/2,\pm\rangle$. The mirror planes σ_v and $\sigma_h=U\sigma_v$ yield new parities for $\mathcal{Z}$ and $\mathcal{A}$ tubes. Even and odd states with respect to σ_v are labeled by A and B. The parity of the horizontal mirror plane σ_h is denoted as that of U, i.e., "+" and "−" now points to the even and odd states with respect to either one of these z-reversing operations. For each $m=1,...,n-1$ and $k \in (0,\pi/a)$ the states $|km\rangle$, $|k,-m\rangle$, $|-km\rangle$, and $|-k,-m\rangle$ form four fold degenerate band. Only for $m=0$, n, when the states posses sharp parity A/B the degeneracy remains twofold: $|km,A/B\rangle$ and $|-km,A/B\rangle$. In $k=0$, the states $|00,\pm,A/B\rangle$ and $|0n,\pm,A/B\rangle$ are nondegenerate, while for the remaining $m=1,...,n-1$, the states $|0m\pm\rangle$ and $|0,-m\pm\rangle$ are double degenerate. At $k=\pi/a$, for integer $m \in (0,n/2)$ the fourfold degenerate states $|\pi m\rangle$, $|\pi,-m\rangle$, $|\pi,n-m\rangle$, and $|\pi,m-n\rangle$ appear, while for $m=0$, n, the states $|\pi 0,A/B\rangle$ and $|\pi n,A/B\rangle$ as well as the states (only for n even) $|\pi,n/2,\pm\rangle$ and $|\pi,-n/2,\pm\rangle$ are double degenerate.

The same quantum numbers may characterize several eigenstates with equal or different eigenenergies. In such cases the index F differing between such states is added. In the considered model for each m there are two electronic bands, with eigenenergies $\epsilon_m^{\pm}(k)$ and the vectors $|km;\pm\rangle$, $|-k,-m;\pm\rangle$ distinguished by $F=\pm$.

The tight binding hamiltonian including a single π orbital $|tsu\rangle$ per site C_{tsu} is

$$H=\sum_{tsu}\sum_{t's'u'} H_{tsu,t's'u'}|tsu\rangle\langle t's'u'|$$

The electronic bands for such a Hamiltonian in the approximation of the nearest neighbors interaction and orthogonal atomic orbitals have been calculated and assigned by k and m only.[2,3] Here, within less crude approximations, we complete the assignation by the additional parities.

It is convenient to introduce the phases

$$\psi_m^k(t,s)=\frac{kan+2\pi mr}{q}t+\frac{2\pi m}{n}s. \tag{4}$$

Then, for the double degenerate E bands of the chiral tube the dispersion relations and the corresponding eigen vectors are obtained solving the eigenproblem of

$$H_m(k)=\begin{pmatrix} h_m^0(k) & h_m^{1*}(k) \\ h_m^1(k) & h_m^0(k)\end{pmatrix}, \tag{5a}$$

$$h_m^u(k)=\sum_{ts} H_{tsu}e^{i\psi_k^m(t,s)} \quad (u=0,1), \tag{5b}$$

with $H_{tsu}=H_{000,tsu}$. For each m one finds two bands

$$\epsilon_m^{\pm}(k)=h_m^0(k)\pm|h_m^1(k)| \tag{6a}$$

with the corresponding generalized Bloch eigenfunctions

$$|km;\pm\rangle=\sum_{ts} e^{-i\psi_m^k(t,s)}(|ts0\rangle\pm e^{ih_m^k}|ts1\rangle),$$

$$|-k,-m;\pm\rangle=\sum_{ts} e^{i\psi_m^k(t,s)}(|ts1\rangle\pm e^{ih_m^k}|ts0\rangle), \tag{6b}$$

where $h_m^k=\mathrm{Arg}[h_m^1(k)]$.

Note that the atoms with $u=0$ and $u=1$ contribute only to the diagonal and off diagonal terms of $H_m(k)$, respectively. Consequently, in the dispersion relations (6a), the interactions of C_{000} with C_{ts0} atoms determine for each k the average energy of two bands, while the interactions with C_{ts1} atoms shifts up and down symmetrically this average to the eigenenergies. This result is not restricted to approximate choice of the interacting neighbors and includes the local distortions induced by the cylindrical geometry. Further, note that $H_{tsu,t's'u'}$ would be equal to $\langle tsu|H|t's'u'\rangle$ if and only if the atomic orbitals $|tsu\rangle$ were orthonormal basis. Since expressed in terms of $H_{tsu,t's'u'}$ matrix elements, Eqs. (6) refer to the realistic nonorthonormal case (therefore the resulting Bloch functions are not orthonormalized). To take advantage of the calculated[9–12] elements $\langle tsu|H|t's'u'\rangle$ and the overlap integrals $\langle 000|tsu\rangle$ one uses another matrix having also the form (5), but with $\langle 000|H|tsu\rangle$ instead of H_{tsu}. Multiplying Eq. (5a) by the inverse of the analogous matrix of the overlap integrals, one gets $H_m(k)$ completely in terms of the known Slater-Koster elements and the overlap integrals.

Also, the result (6a) is general in the sense that the eigenenergies at the edges of the irreducible domain can be obtained from this expression by substituting the limiting values of k numbers; the nondegenerate ones single out the states with U parity. For the $\mathcal{Z}$ and $\mathcal{A}$ tubes the dispersion relations can be derived, too: only $n_1=q/2=n$ and $n_2=0$ for the zig-zag or $n_1=n_2=n$ for the armchair tubes should be used. In these cases Eq. (6a) is the same for m and $-m$, reflecting the anticipated general conclusion that the bands of the achiral tubes are fourfold degenerate apart from the double degenerate $m=0$, n bands. These double degenerate bands are with even σ_v parity for $\mathcal{Z}$ tubes, while they form two pairs with opposite σ_v parity in $\mathcal{A}$ tubes. Nevertheless, the corresponding symmetry adapted vectors in these cases cannot be in general derived from Eq. (6b).

As for the most usual orthogonal orbitals nearest neighbors approximation, the sums in Eq. (5) are restricted to the constant term H_{000} in $h_m^0(k)$ and to the three nearest neighbors in $h_m^1(k)$. Taking $H_{000}=0$, i.e., shifting the energy scale for H_{000}, and substituting in Eq. (4) for the nearest neighbors (Fig. 1) the parameters

$$t_1=-\frac{n_2}{n},\quad s_1=\frac{2n_1+(1+r\mathcal{R})n_2}{q\mathcal{R}},$$

$$t_2=\frac{n_1}{n},\quad s_2=\frac{(1-r\mathcal{R})n_1+2n_2}{q\mathcal{R}},$$

$$t_3=t_1+t_2,\quad s_3=s_1+s_2,$$

one gets for each m the pair of equally assigned bands

$$\epsilon_{Em}^{\pm}(k)=\pm\left|\sum_{i=1}^{3}H_{t_is_i1}e^{i\psi_m^k(t_i,s_i)}\right|. \tag{7}$$

Finally, the rolling up induced differences in the interatomic distances of the honeycomb lattice are frequently neglected (homogeneous distortions approximation), which is achieved by setting $H_{t_is_i1}=V$ for the nearest neighbors (V is estimated between -3.003 and -2.5 eV). All the dispersion relations and the corresponding eigen states (in the form of generalized Bloch sums) are given in the Table I for this approximation, and in Fig. 2 the assignation of these bands for several tubes is presented.

III. SELECTION RULES

One of the most important benefits from the assignation by all quantum numbers comes through the applications of the selection rules in various calculations of physical properties of nanotubes. In fact, each allowed pair (k, m), together with the parities when necessary (Sec. II), singles out one multiplet (irreducible representation). In this sense, a multiplet is specified by $(km\Pi)$, where Π stands for all possible parities. If the multiplet is degenerate (doublets and quadruplets) the "raw" index r running from 1 to its degeneration is used to enumerate its states (with the same eigenenergy). Altogether, the state is denoted as $|km\Pi r;F\rangle$. For example, the symmetry adapted eigenstates of the ${}_kE_m$ electronic bands of $\mathcal{C}$ tubes (Sec. II are now denoted as $|km1;\pm\rangle=|km;\pm\rangle$ and $|km2;\pm\rangle=|-k,-m;\pm\rangle$. Analogously, the quantum numbers are associated to the components $Q_r^{(km\Pi)}$ of the physical tensor Q, giving their transformation rules under the line group symmetry operations. Then, the matrix elements of Q are expressed in the Wigner-Eckart form[13]

$$\begin{aligned}(k_fm_f\Pi_fr_f;F_f|Q_r^{(km\Pi)}|k_im_i\Pi_ir_i;F_i\rangle&\\=\langle k_fm_f\Pi_fr_f|km\Pi,r;k_im_i\Pi_ir_i\rangle&\\\times Q(k_fm_f\Pi_f;F_f\|km\Pi\|k_im_i\Pi_i;F_i).&\end{aligned} \tag{8}$$

Here, $Q(k_fm_f\Pi_f;F_f\|km\Pi\|k_im_i\Pi_i;F_i)$, the reduced matrix element, is independent on the indices r, r_i, and r_f. The Clebsch-Gordan coefficients $\langle k_fm_f\Pi_fr_f|km\Pi r;k_im_i\Pi_ir_i\rangle$, being independent on Q, are *a priori* given by the symmetry of the system; the matrix elements are thus subjected to the selection rules showing when these coefficients are nonzero.

The Clebsch-Gordan coefficients comprise complete information on the selection rules. For the SWCT symmetry groups (1) they are given in the Appendix. Generally they reflect conservation laws of the linear momentum $\Delta k=k_f-k_i\doteq k$ and parities $\Pi_f=\Pi\Pi_i$ (assuming $+1$ for "$+$" or A, and -1 for "$-$" and B). As for the z component of the quasiangular momentum $\Delta m=m_f-m_i\doteq m+Kp$. Here K is integer, which is nonzero in the Umklapp processes (see the Appendix). Whenever Kp is not a multiple of q, m is not conserved quantity; in fact it is related to the isogonal group rotations C_q^s, and only C_n^s among them are symmetries of the nanotube).

The symmetry properties of the most interesting tensors are expressed[14] in terms of the three-dimensional vector representations D^p and D^a (polar and axial) of $\mathbf{L}$, since these tensors are functions of the radius vector $\mathbf{r}$, momentum $\mathbf{p}$, electrical field $\mathbf{E}$ (polar vectors), angular momentum $\mathbf{l}$, and magnetic field $\mathbf{H}$ (axial vectors). The irreducible components of the corresponding representations are given in the Table II. For all of them $k=0$, causing that only direct processes are encountered and now m is also a conserved quantum number (since $k_i=k_f$ yields $K=0$). This means that their symmetry properties are related to the isogonal groups (3).

To facilitate the application of Eq. (8) we discuss the general forms of some of the tensors indicated in Table II being related to the optical properties[15] of nanotubes. In the linear approximation the tensor of the dielectric permeability in the weak external electric field $\mathbf{E}$ is $\varepsilon_{[ij]}(\mathbf{E})=\varepsilon_{[ij]}(0)+\Sigma_k\alpha_{[ij]k}\mathbf{E}_k$. For the chiral tubes, the general form of the zero field permeability tensor[4] is $\varepsilon(0)=\mathrm{diag}(\varepsilon_{xx},\varepsilon_{xx},\varepsilon_{zz})$. As the frequency number of the trivial representation ${}_0A_0^+$ in the $\alpha_{[ij]k}$ is equal to one, the single parameter α, determined by the tube microscopic properties, controls the field-dependent dielectric permeability behavior

$$\varepsilon(\mathbf{E})=\begin{pmatrix}\varepsilon_{xx}&0&\alpha E_y\\0&\varepsilon_{xx}&-\alpha E_x\\\alpha E_y&-\alpha E_x&\varepsilon_{zz}\end{pmatrix}.$$

Thus, the optical activity of $\mathcal{C}$ tubes is changed by the perpendicular electric field, and instead of one there are two optic axes whose direction depend on the applied field. For the $\mathcal{Z}$ and $\mathcal{A}$ tubes the external field does not change their optical symmetry, since no trivial component appears in the decomposition.

The electromagnetic response to a weak applied field is characterized by the dielectric function $\varepsilon_{ij}(\mathbf{k},\omega)$. Although optical absorption and diffraction are well described within the long-wavelength limit, for the optical activity the terms of ε_{ij} linear in the components of the wave vector $\mathbf{k}$ (having different symmetry from the $\mathbf{k}$-independent ones) should be considered. These linear terms define the tensor γ_{ijk} and its symmetric and antisymmetric[16] parts with respect to the last two subscripts $\gamma_{ijk}=[\partial\varepsilon_{ij}(\mathbf{k},\omega)/\partial k_l]_{\mathbf{k}=0}=i(\gamma_{i\{jl\}}^A+\gamma_{i[jl]}^S)$. For the $\mathcal{Z}$ and $\mathcal{A}$ tubes there is no linear optical response

TABLE I. Bands and symmetry-adapted eigenvectors of the carbon nanotubes. For each irreducible representation the corresponding frequency number N, energy ϵ in the simplest (orthogonal orbitals, nearest neighbors, homogeneous distortions) model, and generalized Bloch functions $|km\Pi\rangle$ of the corresponding bands are given. $\gamma=\mathrm{Arg}[V+2Ve^{\mathrm{ika}/2}\cos(\pi m/n)]$.

$\mathcal{C}$	N	ϵ	Generalized Bloch functions
${}_0A_m^{\Pi}$	1	$V\Pi(1+2c^{2i(m\pi/q)})$	$\lvert m\Pi\rangle=\frac{1}{\sqrt{\lvert L_{\mathcal{C}}\rvert}}\sum_{ts} e^{-i\psi_m^0(t,s)}(\lvert ts0\rangle+\Pi\lvert ts1\rangle)$
${}_{\pi}A_m^{\Pi}$	1	$-V\Pi$	$\lvert \pi m\Pi\rangle=\frac{1}{\sqrt{\lvert L_{\mathcal{C}}\rvert}}\sum_{ts} e^{-i\psi_m^{\pi}(t,s)}(\lvert ts0\rangle+\Pi\lvert ts1\rangle)$
${}_kE_m$	2	$\pm\lvert V\Sigma_i e^{i\psi_m^k(t_i,s_i)}\rvert$	$\lvert km;\pm\rangle=\frac{1}{\sqrt{\lvert L_{\mathcal{C}}\rvert}}\sum_{ts} e^{-i\psi_m^k(t,s)}(\lvert ts0\rangle\pm e^{ih_m^k}\lvert ts1\rangle)$
			$\lvert -k,-m;\pm\rangle=\frac{1}{\sqrt{\lvert L_{\mathcal{C}}\rvert}}\sum_{ts} e^{i\psi_m^k(t,s)}(\lvert ts1\rangle\pm e^{ih_m^k}\lvert ts0\rangle)$
$\mathcal{Z}$	N	ϵ	Generalized Bloch functions
${}_0A_m^{\Pi}$	1	$V\Pi(1+2e^{i(m\pi/n)})$	$\lvert 0m\Pi A\rangle=\sqrt{\frac{2}{\lvert L_{\mathcal{Z}}\rvert}}\sum_{ts} e^{-i(m\pi/n)\,t}(\lvert ts0\rangle+\Pi\lvert ts1\rangle)$
${}_0E_m^{\Pi}$	1	$V\Pi\left(1+2\cos\frac{m\pi}{n}\right)$	$\lvert 0m\Pi\rangle=\sqrt{\frac{2}{\lvert L_{\mathcal{Z}}\rvert}}\sum_{ts} e^{-i(m\pi/n)\,(2s+t)}(\lvert ts0\rangle+\Pi e^{i(2m\pi/n)}\lvert ts1\rangle)$
			$\lvert 0,-m,\Pi\rangle=\sqrt{\frac{2}{\lvert L_{\mathcal{Z}}\rvert}}\sum_{ts} e^{i(m\pi/n)\,(2s+t)}(e^{i(2m\pi/n)}\lvert ts0\rangle+\Pi\lvert ts1\rangle)$
${}_kE_m^A$	2	$\pm\lvert V\rvert\sqrt{5+4e^{i(m\pi/n)}\cos\frac{ka}{2}}$	$\lvert kmA;\pm\rangle=\sqrt{\frac{2}{\lvert L_{\mathcal{Z}}\rvert}}\sum_{ts} e^{-i((m\pi/n)+(ka/2))t}(\lvert ts0\rangle\pm e^{ih_m^k}\lvert ts1\rangle)$
			$\lvert -k,m,A;\pm\rangle=\sqrt{\frac{2}{\lvert L_{\mathcal{Z}}\rvert}}\sum_{ts} e^{-i((m\pi/n)-(ka/2))t}(\lvert ts1\rangle\pm e^{ih_m^h}\lvert ts0\rangle)$
${}_{\pi}E_{n/2}^{\Pi}$	1	$-V\Pi$	$\left\lvert \pi,\frac{n}{2},\Pi\right\rangle=\sqrt{\frac{2}{\lvert L_{\mathcal{Z}}\rvert}}\sum_{ts}(-1)^{s+t}(\lvert ts0\rangle+\Pi\lvert ts1\rangle)$
			$\left\lvert \pi,-\frac{n}{2},\Pi\right\rangle=\sqrt{\frac{2}{\lvert L_{\mathcal{Z}}\rvert}}\sum_{ts}(-1)^{s}(\lvert ts0\rangle+\Pi\lvert ts1\rangle)$
${}_kG_m$	2	$\pm\lvert V\rvert\sqrt{1+4\cos\frac{ka}{2}\cos\frac{m\pi}{n}+4\cos^2\frac{m\pi}{n}}$	$\lvert km;\pm\rangle=\sqrt{\frac{2}{\lvert L_{\mathcal{Z}}\rvert}}\sum_{ts} e^{-i(ka/2)t}e^{-i(m\pi/n)(t+2s)}(\lvert ts0\rangle\pm e^{i\gamma}e^{i(2m\pi/n)}\lvert ts1\rangle)$
			$\lvert k,-m;\pm\rangle=\sqrt{\frac{2}{\lvert L_{\mathcal{Z}}\rvert}}\sum_{ts} e^{-i(ka/2)t}e^{i(m\pi/n)(t+2s)}(e^{i(2m\pi/n)}\lvert ts0\rangle\pm e^{i\gamma}\lvert ts1\rangle)$
			$\lvert -k,m;\pm\rangle=\sqrt{\frac{2}{\lvert L_{\mathcal{Z}}\rvert}}\sum_{ts} e^{i(ka/2)t}e^{-i(m\pi/n)(t+2s)}(e^{i(2m\pi/n)}\lvert ts1\rangle\pm e^{i\gamma}\lvert ts0\rangle)$
			$\lvert -k,-m;\pm\rangle=\sqrt{\frac{2}{\lvert L_{\mathcal{Z}}\rvert}}\sum_{ts} e^{i(ka/2)t}e^{i(m\pi/n)(t+2s)}(\lvert ts1\rangle\pm e^{i\gamma}e^{i(2m\pi/n)}\lvert ts0\rangle)$
$\mathcal{A}$	N	ϵ	Generalized Bloch functions
${}_0\Pi_m^+$	1	$V\Pi(1+2e^{i(m\pi/n)})$	$\lvert 0m+\Pi\rangle=\sqrt{\frac{2}{\lvert L_{\mathcal{A}}\rvert}}\sum_{ts} e^{-i(m\pi/n)t}(\lvert ts0\rangle+\Pi\lvert ts1\rangle)$
${}_0E_m^+$	2	$\pm\lvert V\rvert\sqrt{5+4\cos\frac{m\pi}{n}}$	$\lvert 0m+;\pm\rangle=\sqrt{\frac{2}{\lvert L_{\mathcal{A}}\rvert}}\sum_{ts} e^{-i(m\pi/n)(2s+t)}(\lvert ts0\rangle\pm e^{ih_m^0}\lvert ts1\rangle)$
			$\lvert 0,-m,+;\pm\rangle=\sqrt{\frac{2}{\lvert L_{\mathcal{A}}\rvert}}\sum_{ts} e^{i(m\pi/n)(2s+t)}(\lvert ts1\rangle\pm e^{ih_m^0}\lvert ts0\rangle)$

TABLE I. (*Continued*).

$\mathcal{A}$	N	ϵ	Generalized Bloch functions
${}_kE_m^{\Pi}$	1	$V\Pi\left(1+2e^{i(m\pi/n)}\cos\frac{ka}{2}\right)$	$\lvert km\Pi\rangle=\sqrt{\frac{2}{\lvert L_{\mathcal{A}}\rvert}}\sum_{ts} e^{-i((m\pi/n)+(ka/2))t}(\lvert ts0\rangle+\Pi\lvert ts1\rangle)$
			$\lvert -k,m,\Pi\rangle=\sqrt{\frac{2}{\lvert L_{\mathcal{A}}\rvert}}\sum_{ts} e^{-i((m\pi/n)-(ka/2))t}(\lvert ts0\rangle+\Pi\lvert ts1\rangle)$
${}_{\pi}E_{n/2}^{\Pi}$	1	$-V\Pi$	$\left\lvert \pi,\frac{n}{2},\Pi\right\rangle=\sqrt{\frac{2}{\lvert L_{\mathcal{A}}\rvert}}\sum_{ts}(-1)^{s+t}(\lvert ts0\rangle+\Pi\lvert ts1\rangle)$
			$\left\lvert \pi,-\frac{n}{2},\Pi\right\rangle=\sqrt{\frac{2}{\lvert L_{\mathcal{A}}\rvert}}\sum_{ts}(-1)^{s}(\Pi\lvert ts0\rangle+\lvert ts1\rangle)$
${}_kG_m$	2	$\pm\lvert V\rvert\sqrt{1+4\cos\frac{ka}{2}\cos\frac{m\pi}{n}+4\cos^2\frac{ka}{2}}$	$\lvert km;\pm\rangle=\sqrt{\frac{2}{\lvert L_{\mathcal{A}}\rvert}}\sum_{ts} e^{-i(ka/2)t}e^{-i(m\pi/n)(t+2s)}(\lvert ts0\rangle\pm e^{ih_m^k}\lvert ts1\rangle)$
			$\lvert k,-m;\pm\rangle=\sqrt{\frac{2}{\lvert L_{\mathcal{A}}\rvert}}\sum_{ts} e^{-i(ka/2)t}e^{i(m\pi/n)(t+2s)}(\lvert ts1\rangle\pm e^{ih_m^k}\lvert ts0\rangle)$
			$\lvert -k,m;\pm\rangle=\sqrt{\frac{2}{\lvert L_{\mathcal{A}}\rvert}}\sum_{ts} e^{i(ka/2)t}e^{-i(m\pi/n)(t+2s)}(\lvert ts0\rangle\pm e^{ih_m^k}\lvert ts1\rangle)$
			$\lvert -k,-m;\pm\rangle=\sqrt{\frac{2}{\lvert L_{\mathcal{A}}\rvert}}\sum_{ts} e^{i(ka/2)t}e^{i(m\pi/n)(t+2s)}(\lvert ts1\rangle\pm e^{ih_m^k}\lvert ts0\rangle)$

while for the chiral tubes the antisymmetric part $\gamma^A_{i\{jl\}}$ is determined by two independent parameters involved in six nonvanishing tensor elements $\gamma^A_{xyz}=\gamma^A_{yzx}=-\gamma^A_{xzy}=-\gamma^A_{yxz}$ are related to the interband transitions ${}_0A_0^{\pm}\leftrightarrow{}_0E_1$, ${}_kE_m\leftrightarrow{}_kE_{m+1}$ $(k\in[0,\pi])$, ${}_0A_{q/2}\leftrightarrow{}_0E_{q/2-1}$ [this follows from Eq. (8) when the operators p_x, p_y, l_x, and l_y are substituted for Q], while $\gamma^A_{zxy}=-\gamma^A_{zyx}$ are related to the interband transitions ${}_0A_0^{\pm}\leftrightarrow{}_0A_0^{\mp}$ and ${}_0A_{q/2}^{\pm}\leftrightarrow{}_0A_{q/2}^{\mp}$ (now p_z and l_z are used). The single independent parameter of $\gamma^S_{i[jl]}$ is involved in the four nonvanishing tensor elements: $\gamma^S_{xyz}=\gamma^S_{xzy}=-\gamma^S_{yxz}=-\gamma^S_{yzx}$ related to the interband transitions induced by the symmetric operator $\frac{1}{2}(\hat{z}\hat{p}_y+\hat{y}\hat{p}_z+\text{H.c.})$.

The conductivity tensor σ_{ij} of a system in a sufficiently weak magnetic field $\mathbf{H}$ is well approximated quadratically:

$$\sigma_{ij}(\mathbf{H})=\sigma_{[ij]}(0)+\sum_{k=1}^{3}\rho_{\{ij\}k}H_k+\sum_{k=1}^{3}\sum_{l=1}^{3}\beta_{[ij][kl]}H_kH_l,$$

where the symmetry [4,17] allows a symmetric tensor $\sigma_{[ij]}(0)=\mathrm{diag}(\sigma_{xx},\sigma_{xx},\sigma_{zz})$. The third rank tensor $\rho_{\{ij\}k}$ is responsible for the linear contribution of the field (Hall effect), while the fourth rank tensor $\beta_{[ij][kl]}$ introduces a small correction to the main effect. Because of the symmetry, $\rho_{\{ij\}k}$ is of the same form for all SWCT's ($\mathcal{C}$, $\mathcal{Z}$, $\mathcal{A}$): two independent parameters ρ_1 and ρ_2 define its six nonvanishing tensor components $\rho_{xyz}=-\rho_{yxz}=\rho_1$, $\rho_{xzy}=-\rho_{zxy}=\rho_{zyx}=-\rho_{zxy}=\rho_2$. Also $\beta_{[ij][kl]}$ is of the same form for the chiral and the achiral SWCT, with six independent parameters involved within altogether 21 nonzero components $\beta_{xxxx}=\beta_{yyyy}$

TABLE II. Symmetry of the tensors of SWCT's. The decompositions onto irreducible representations of the most frequent tensors (given in the last column) of the chiral (column 2) and the zig-zag and the armchair (column 3) SWCT's. Tensors are obtained by multiplying polar and axial vectors, and the type of the products ($\otimes$, $[\cdots]$ and $\{\cdots\}$ for the direct, symmetrized, and antisymmetrized) is in the first column.

Type	$\mathcal{C}$ tubes	$\mathcal{Z}$ and $\mathcal{A}$ tubes	Tensor
D^p	${}_0A_0^-+{}_0E_1$	${}_0A_0^-+{}_0E_1^+$	r_i,p_i,E_i
$D^a=\{D^{a/p^2}\}$	${}_0A_0^-+{}_0E_1$	${}_0B_0^++{}_0E_1^-$	$l_i,H_i,R_{\{ij\}}$
D^{a/p^2}	$2{}_0A_0^++{}_0A_0^-+2{}_0E_1+{}_0E_2$	$2{}_0A_0^++{}_0B_0^++2{}_0E_1^-+{}_0E_2^+$	$\rho_{\{ij\}k},R_{ij}$
$[D^{a/p^2}]$	$2{}_0A_0^++{}_0E_1+{}_0E_2$	$2{}_0A_0^++{}_0E_1^-+{}_0E_2^+$	$\epsilon_{[ij]},\sigma_{[ij]},R_{[ij]}$
$D^p\otimes D^a$	$2{}_0A_0^++{}_0A_0^-+2{}_0E_1+{}_0E_2$	${}_0A_0^-+2{}_0B_0^-+2{}_0E_1^++{}_0E_2^-$	$\gamma^A_{i\{jk\}}$
$D^p\otimes[D^{a/p^2}]$	${}_0A_0^++3{}_0A_0^-+4{}_0E_1+2{}_0E_2+{}_0E_3$	$3{}_0A_0^-+{}_0B_0^-+4{}_0E_1^++2{}_0E_2^-+{}_0E_3^+$	$\alpha_{[ij]k},\gamma^S_{i[jl]}$
D^{p^3}	$3{}_0A_0^++4{}_0A_0^-+6{}_0E_1+3{}_0E_2+{}_0E_3$	$4{}_0A_0^-+3{}_0B_0^-+6{}_0E_1^++3{}_0E_2^-+{}_0E_3^+$	γ_{ijk}
$[D^{a/p^2}]\otimes[D^{a/p^2}]$	$6{}_0A_0^++2{}_0A_0^-+6{}_0E_1+5{}_0E_2+2{}_0E_3+{}_0E_4$	$6{}_0A_0^++2{}_0B_0^++6{}_0E_1^-+5{}_0E_2^++2{}_0E_3^-+{}_0E_4^+$	$\beta_{[ij][kl]}$

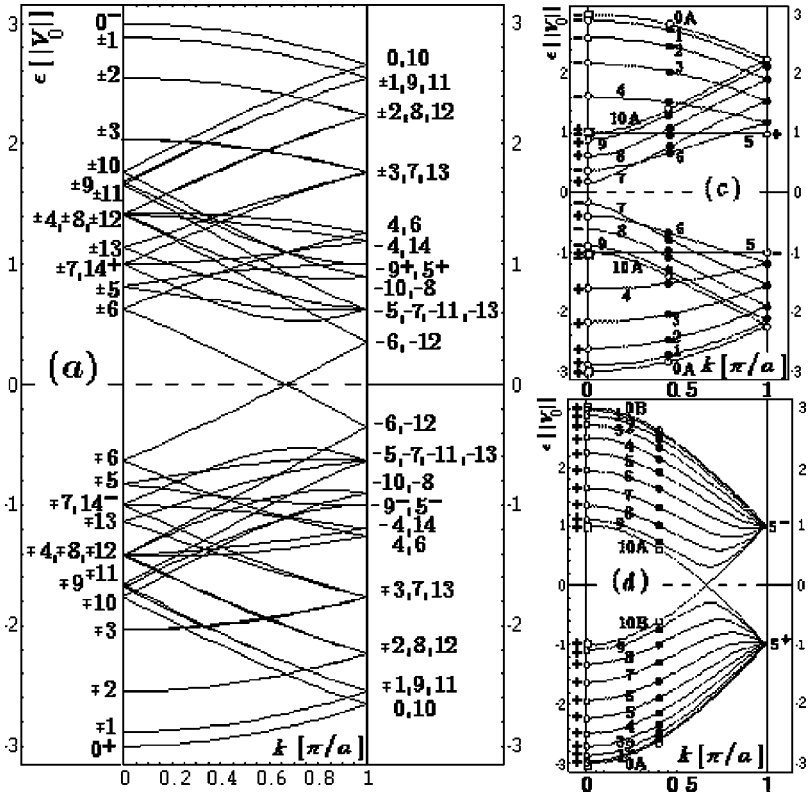

FIG. 2. Symmetry assigned electronic bands of SWCT's. (a) For the chiral tube (8, 2) (line group $\mathbf{T}_{28}^{11}\mathbf{D}_2=\mathbf{L}28_{18}22$, $a=\sqrt{7}a_0=6.5\,\text{Å}$) the bands are double degenerate in the interior of ID while at the edges + or − emphasize the *U*-parity of singlets; *m* is given at the both edges of the band. (b) and (c): The bands of the zig-zag (10, 0) and the armchair (10, 10) tubes (line group $\mathbf{T}_{20}^{1}\mathbf{D}_{10h}=\mathbf{L}20_{10}/mcm$, $a_{\mathcal{Z}}=\sqrt{3}a_0=4.26\,\text{Å}$, and $a_{\mathcal{A}}=a_0$) are either fourfold (${}_kG_m$,●) or double degenerate (${}_kE_{0/10}^{A/B}$, ○, σ_v parity *A* or *B* given next to *m*); *z*-reversal parity (+ or −) and nondegenerate states (box) appear at the edges of ID.

$=\beta_1$, $\beta_{zzzz}=\beta_2$, $\beta_{xxyy}=\beta_{yyxx}=\beta_3$ $\beta_{xyxy}=\beta_{xyyx}=\beta_{yxxy}=\beta_{yxyx}=\frac{1}{2}(\beta_1-\beta_3)$, $\beta_{xxzz}=\beta_{yyzz}=\beta_4$, $\beta_{xzxz}=\beta_{xzzx}=\beta_{yzyz}=\beta_{yzzy}=\beta_{zxxz}=\beta_{zxzx}=\beta_{zyyz}=\beta_{zyzy}=\beta_5$, $\beta_{zzxx}=\beta_{zzyy}=\beta_6$. So, the conductivity tensor σ of SWCT's in the presence of the weak magnetic field **H**, up to the square terms in the applied field, is of the form

$$\sigma(\mathbf{H})=\sigma+\begin{pmatrix}\beta_1H_x^2+\beta_3H_y^2+\beta_4H_z^2 & \rho_1H_z+(\beta_1-\beta_3)H_xH_y & \rho_2H_y+2\beta_5H_xH_z\\ -\rho_1H_z+(\beta_1-\beta_3)H_xH_y & \beta_3H_x^2+\beta_1H_y^2+\beta_4H_z^2 & -\rho_2H_x+2\beta_5H_yH_z\\ -\rho_2H_y+2\beta_5H_xH_z & \rho_2H_x+2\beta_5H_yH_z & \beta_6(H_x^2+H_y^2)+\beta_2H_z^2\end{pmatrix}.$$

In general, the Raman (polarizability) tensor R_{ij} relates induced polarization to the external electric field[18] $P_i=\Sigma_jR_{ij}E_j$. Therefore, Table II combined with Eq. (A2) gives the selection rules of the Raman scattering: the relevant transitions are between the states with *km* numbers $k_f-k_i=0$ and $\Delta m=m_f-m_i=0,\pm1,\pm2$; for the achiral tubes *z*-reversal parity of these states is different if $\Delta m=1$ and same if Δm even. For the frequently important symmetric part $R_{[ij]}$ and its anisotropic component $R_{[ij]}^a$ (the last one transforms according to $[D^{p^2}]-{}_0A_0^+$), the momenta selection rules are same, while both the *z* reversal (and the vertical mirror for achiral tubes) parity is conserved if $\Delta m=0$. The isotropic component $R_{[ij]}^s$ transforms according to the identity representation ${}_0A_0^+$, and involves only the transitions between the states with the coincident quantum numbers. As for the antisymmetric part $R_{\{ij\}}$, $\Delta m=0,\pm1$; if $\Delta m=0$ the relevant transitions are between the states with opposite *U*-parity for the chiral tubes and equal horizontal mirror parity but the opposite vertical mirror parity in the achiral cases. Of course, in the concrete calculations, these rules can be further specified according to the incident light polarization and direction.

IV. CONCLUDING REMARKS

The assignation of the energy bands of SWCT's by the complete set of the symmetry based quantum numbers is discussed. Parametrized by the quasimomentum *k*, the bands carry the quantum number of the angular momentum *m*, and parities ± and *A*/*B*, related to specific symmetries of SWCT's. The ranges of *m* has been redefined compared to the one used in the nanotube literature[2] to get the standard quantum mechanical interpretation of the *z* projection of the orbital angular momentum. The momenta quantum numbers are imposed by the rototranslational subgroup $\mathbf{L}^{(1)}=\mathbf{T}_r^q\mathbf{C}_n$,

and characterize all the quasi-1D crystals. Indeed, in their symmetry $\mathbf{L}^{(1)}$ is always present as the maximal abelian part, thus causing no degeneracy. Additional U and σ_v parties of SWCT's introduce band degeneracy. Relating the quantum numbers to the irreducible representations of the symmetry groups this assignation immediately gives the band degeneracies and information on nonaccidental band sticking.

The bands have specific symmetry with respect to the $k=0$ and $k=\pi/a$; therefore, the domain sufficient to characterize the entire band is the non-negative half of the Brillouin zone $[0,\pi]$. At the edge points $k=0$, π/a, either the band stick to the another one or the corresponding eigenstate gets z-reversal parity $\pm$. The U-axis symmetry reverses both the linear and angular momenta causing at least double degeneracy of the bands within $(0, \pi)$. For the $\mathcal{Z}$ and $\mathcal{A}$ tubes, the vertical mirror plane implies degeneracy of m and $-m$ bands. Thus the bands are fourfold degenerate, except $m=0$, n ones, which are σ_v odd or even and double degenerate.

At $k=0$ m and $-m$ bands are sticked together. The screw axis imposes additional band sticking, most easily revealed by the relations between the km-quantum numbers used here, and $\tilde{k}\tilde{m}$ ones alternatively considered in the literature.[3] Namely, the bands $\pm m$ are sticked together at $k=0$, as well as the bands m and $m+p$ at π/a. Altogether, the set of q/n km bands are continued in a single $\tilde{k}\tilde{m}$ band. Further, it can be shown that only the bands ending up with U-parity even or odd states are not sticked to the another ones, with the van Hove singularities and the halved degeneracy at their end points. These are general topological properties of any (quasi) particle energy bands of SWCT's. All other bands sticking or increased degeneracy, if any, are accidental, i.e., related to the Hamiltonian under study. Note that only within spin independent models the U axis imposed double degeneracy coincides with that introduced by the time reversal symmetry, since both operations reverse linear and orbital angular momenta.

According to this general scheme the complete assignation of the SWCT electronic tight-binding bands is performed. The generalized Bloch functions are found and characterized by the full set of $(km\Pi)$ quantum numbers. All these functions contain two parts: the two halves of SWCT consisting of C_{ts0} and C_{ts1} atoms (black and white ones in the Fig. 1) contribute to the state by different phase factors. This form is useful in calculations and comparison to the STM images,[19] again manifests the existence of the U symmetry which interrelate the two halves.

A brief comment on the SWCT conductivity within the present context may enlighten some of the discussed questions. Recall that the simplest (tight-binding nearest neighbors and homogeneous distortions) model with the bands given in the Table I, predicts[2,3] that the tubes with n_1-n_2 divisible by 3 should be conductors due to the crossing[20] of the two bands m_F at k_F: when $\mathcal{R}=3$ then $k_F=2\pi/3$ and $m_F=nr \pmod{q}$, while $k_F=0$ and $m_F=\pm q/3$ for $\mathcal{R}=1$. This extra degeneracy at the Fermi level is a model dependent accidental one, being not induced by symmetry. On the contrary, the symmetry based noncrossing rule prevents the conductivity except in the armchair tubes, since the momenta quantum numbers of the crossing bands are the same; only for the armchair tubes, when $m_F=n$ these bands also carry the opposite vertical mirror parity. So, as verified experimentally[21] and in the more subtle theoretical models,[20] the secondary gap must be opened except for the armchair tubes, for which the accidental crossing point k_F is shifted to the left. In these cases the metallic plato[19,22] is ended by the systematic van Hove singularities.

The major benefit from the complete assignation of bands and corresponding generalized Bloch functions comes from the selection rules. The momenta conservation selection rules (A1) emerge from the rototranslational subgroup $\mathbf{T}_q^r\mathbf{C}_n$ making these rules also applicable to all other nanotubes (multiwall, BN, etc.) and stereoregular polymers. The novel conserved parities refine the momenta conservation rules. The coincidence of the z-reversal odd and even states with the systematic van Hove singularities proves substantial influence of the parities to the physical processes in nanotubes and related spectra.[16,23] Therefore, these additional rules must not be overlooked in calculations.

To illustrate further the relevance of the derived parity selection rules, let us briefly discuss armchair tubes and the parallel component of the dielectric tensor $\epsilon_{ij}(\mathbf{k},\omega)$, which is the corner stone in the analysis of various optical properties.[16] The contribution of the direct interband transitions caused by the electric field along the z axis are to be included in calculations. As the perturbation field has odd z reversal and even vertical mirror parities, it transforms according to the representation ${}_0A_0^-$. Therefore, the absorption may be realized only by the (vertical) transitions $\epsilon_m^-(k) \rightarrow \epsilon_m^+(k)$, and this exhausts the selection rules imposed by the rototranslational subgroup. Nevertheless, the eigen states of the pairs of the double degenerate bands with $m=0$, n have different σ_v parity, and the transitions between these bands are forbidden for any k. Thus, only the transitions between the fourfold degenerate ${}_kG_m$ bands are allowed for z polarized light. Also in the Raman scattering processes the selection rules besides the momenta strongly involve parities.

Finally, the tensor properties of some physical quantities were established, to make the use of the selection rules quite straightforward. We emphasize that the considered tensors interrelate vector (polar or axial) quantities making that all of them are associated to quantum number $k=0$. This provides full conservation of momenta (e.g., vertical optical transitions), although in general m is not conserved.

APPENDIX: CLEBSCH-GORDAN COEFFICIENTS

The Clebsch-Gordan coefficients are given for the irreducible representations of the line groups $\mathbf{L}_\mathcal{C}$ and $\mathbf{L}_\mathcal{A}$ presented in Ref. 7. These coefficients reflect the conservation laws of z components of the linear and angular quasi momenta, as well as of the parities with respect to the U axis and the mirror planes σ_v or σ_h. The addition of quasimomenta is performed modulo their range, which is indicated by $\doteq$:

$$k+k_i \doteq k+k_i+2K\pi/a, \tag{A1a}$$

$$m+m_i \doteq m+m_i+Mq, \tag{A1b}$$

where K and M are the integers providing the results in $(-\pi/a,\pi/a]$ and $(-q/2,q/2]$, respectively. In the following expressions the value of the parities Π may be ± 1 for even and odd states or 0 for all the other states with undefined parity. When this value is explicitly given (or absent) in expression, all the other quantum numbers are restricted to the compatible values. For given values (k,m,Π) and (k_i,m_i,Π_i), the Clebsch-Gordan coefficients are nonvanishing only if $k_f \doteq = k+k_i$ and $m_f \doteq m+m_i+pK$, where $K=(k+k_i-k_f)a/2\pi$ is an integer, and $\Pi_f=\Pi\Pi_i$ when both Π and Π_i are defined. For $\mathcal{Z}$ and $\mathcal{A}$ tubes $p=n$ and $\Pi_f=\Pi\Pi_i$ refers to conservation of each parities separately. In all these cases the value of the CG coefficient is 1,

$$\langle k_f,m_f,\Pi_f|km\Pi;k_im_i\Pi_i\rangle=1, \tag{A2}$$

with the following exceptions.

(1) Chiral tubes:

$$\langle k_f,m_f|km;k_im_i-\rangle=-1, \text{ if } k<0, \text{ or } k=0, \quad m<0, \text{ or } k=\pi/a, \ m\notin\left[-\frac{p}{2},\frac{q-p}{2}\right],$$

$$\langle k_f,m_f|km-;k_im_i\rangle=-1, \text{ if } k_i<0, \text{ or } k_i=0, \ m_i<0, \text{ or } k_i=\pi/a, \ m_i\notin\left[-\frac{p}{2},\frac{q-p}{2}\right],$$

$$\langle k_f,m_f,\pm|k,m;k_i,m_i\rangle=\begin{cases}\pm\dfrac{1}{\sqrt{2}}, & k<0, \text{ or } k=0, \quad m<0 \text{ or } k=\pi, \ m_i\notin\left[-\dfrac{p}{2},\dfrac{q-p}{2}\right],\\ \dfrac{1}{\sqrt{2}}, & \text{otherwise.}\end{cases} \tag{A3}$$

(2) Achiral tubes (only the cases with $k=0$ are considered; θ_x is the negative step function, being 1 when $x<0$ and zero otherwise; especially θ_{Π^s} is shorten to θ_s, for $s=h,\ v,\ U$):

$$\langle 0,m_f,\Pi^h\Pi^{h_i}|0,m,B,\Pi^h;0,m_i,\Pi^{h_i}\rangle=-1, \text{ if } m_i<0,$$

$$\langle 0,m_f,\Pi^h\Pi^{h_i}|0,m,\Pi^h;0,m_i,B,\Pi^{h_i}\rangle=-1, \text{ if } m<0,$$

$$\langle 0,m_f,\Pi^v\Pi^{v_i}|0,m,\Pi^v,-;k_i,m_i,\Pi^{v_i}\rangle=\langle k_i,m_f|0,m,-;k_i,m_i\rangle=-1, \text{ if } k_i<0,$$

$$\langle \pi/a,m_f,-\Pi^h\Pi^{U_i}|0,m,B,\Pi^h;\pi/a,-n/2,\Pi^{U_i}\rangle=-1;$$

$$\langle k_f,m_f|0,m,\Pi^v,\Pi^h;k_i,m_i\rangle=\langle k_f,m_f|0,m,\Pi^h;k_i,m_i\rangle=(-1)^{\theta_h\theta_{k_i}+\theta_v\theta_{m_i}},$$

$$\langle \pi/a,m_f|0,m\Pi^h;\pi/a,m_i,\Pi^{U_i}\rangle=(-1)^{(\theta_h+\theta_{U_i})(\theta_m+\theta_{m_i})},$$

$$\langle 0,m_f,\Pi^v,\Pi^h\Pi^{h_i}|0,m,\Pi^h;0,m_i,\Pi^{h_i}\rangle=\frac{(-1)^{\theta_v\theta_m}}{\sqrt{2}}, \tag{A4}$$

$$\left\langle \frac{\pi}{a},m_f,\Pi^{U_f}\middle|0,m,\Pi^h;k_i,0,\Pi^{v_i}\right\rangle=\frac{(-1)^{(\theta_{U_f}+\theta_h)\theta_{k_i}+\theta_{v_i}\theta_m}}{\sqrt{2}},$$

$$\left\langle k_f,0,\Pi^{v_f}\middle|0,m,\Pi^h;\frac{\pi}{a},m_i;\Pi^{U_i}\right\rangle=\frac{(-1)^{(\theta_{U_i}+\theta_h)(\theta_{m_i}+\theta_m)+\theta_{v_f}\theta_m}}{\sqrt{2}}$$

$$\langle k_f,m_f,\Pi^{v_f}|0,m,\Pi^h;k_i,m_i\rangle=\frac{(-1)^{\theta_h\theta_{k_i}+\theta_{v_f}\theta_m}}{\sqrt{2}},$$

$$\langle k_f,m_f,\Pi^{U_f}|0,m,\Pi^h;k_i,m_i\rangle=\frac{(-1)^{(\theta_{U_f}+\theta_h)\theta_{k_i}}}{\sqrt{2}}.$$

*Electronic address: tanja37@afrodita.rcub.bg.ac.yu; URL: http://www.ff.bg.ac.yu/qmf/qsg_e.htm

[1] S. Iijima, Nature (London) **354**, 56 (1991).

[2] N. Hamada, S. Sawada, and A. Oshiyama, Phys. Rev. Lett. **68**, 1579 (1992); M. Dresselhaus, G. Dresselhaus, and P. C. Eklund, *Science of Fullerenes and Carbon Nanotubes* (Academic, San Diego, 1998); R. Saito, G. Dresselhaus, and M. Dresselhaus, *Physical Properties of Carbon Nanotubes* (Imperial College Press, London, 1998).

[3] C. T. White, D. H. Robertson, and J. W. Mintmire, Phys. Rev. B **47**, 5485 (1993); C. T. White and T. N. Todorov, Nature (London) **323**, 240 (1998); R. A. Jishi, L. Venkataraman, M. S. Dresselhaus, and G. Dresselhaus, Phys. Rev. B **51**, 11 176 (1995).

[4] M. Damnjanović, I. Milošević, T. Vuković, and R. Sredanović, Phys. Rev. B **60**, 2728 (1999); J. Phys. A **32**, 4097 (1999).

[5] Note that for SWCT $\tilde{q}=q/n=2$ (mod 12) is even; for $\mathcal{Z}$ and $\mathcal{A}$ tubes $\tilde{q}=2$. Since n is also the greatest common divisor of q and p, n and p are simultaneously even only when both n_1 and n_2 are even.

[6] S. L. Altmann, *Band Theory of Solids. An Introduction from the Point of View of Symmetry* (Clarendon, Oxford, 1991); S. S. L. Altmann, *Induced Representations in Crystals and Molecules* (Academic, London, 1977); J. P. Elliot and P. G. Dawber, *Symmetry in Physics* (Macmillan, London, 1979).

[7] M. Damnjanović, T. Vuković, and I. Milošević, J. Phys. A **33**, 6561 (2000).

[8] I. Milošević and M. Damnjanović, Phys. Rev. B **47**, 7805 (1993).

[9] J. C. Slater and G. F. Koster, Phys. Rev. **94**, 1498 (1954).

[10] R. R. Sharma, Phys. Rev. B **19**, 2813 (1979).

[11] H. Eschrig, Phys. Status Solidi B **96**, 329 (1979).

[12] D. Porezag, Th. Frauenheim, Th. Köhler, G. Seifert, and R. Kaschner, Phys. Rev. B **51**, 12 947 (1995).

[13] A. Messiah, *Quantum Mechanics* (North-Holland, Amsterdam, 1972).

[14] W. A. Wooster, *Tensors and Group Theory for the Physical Properties of Crystals* (Clarendon, Oxford, 1973); J. F. Nye, *Physical Properties of Crystals* (Clarendon, Oxford, 1964).

[15] L. D. Landau and E. M. Lifshic, *Electrodynamics of Continuous Media* (Pergamon, London, 1963).

[16] S. Tasaki, K. Maekawa, and T. Yamabe, Phys. Rev. B **57**, 9301 (1998).

[17] M. Damnjanović, Phys. Lett. A **94**, 337 (1983); I. Milošević, *ibid.* **204**, 63 (1995).

[18] M. Cardona, in *Light Scattering in Solids II*, edited by M. Cardona and G. Güntherodt (Springer, Berlin, 1982).

[19] A. Rubio, Appl. Phys. A: Mater. Sci. Process. **68**, 275 (1999); A. Rubio, D. Sanchez-Portal, E. Artacho, P. Ordejon, and J. M. Soler, Phys. Rev. Lett. **82**, 3520 (1999).

[20] C. Kane and E. J. Mele, Phys. Rev. Lett. **78**, 1932 (1997). M. Damnjanović, T. Vuković, and I. Milosević, Solid State Commun. **116**, 265 (2000).

[21] C. Zhou, J. Kong, and H. Dai, Phys. Rev. Lett. **84**, 5604 (2000).

[22] Ph. Lambin, V. Meunier, and A. Rubio, Phys. Rev. B **62**, 5129 (2000).

[23] J. C. Charlier and Ph. Lambin, Phys. Rev. B **57**, R15 037 (1998); S. Reich and C. Thomsen, *ibid.* **62**, 4273 (2000).